Faculty of Enigeering

Cairo University

Antenna Engineering

ELC 3050 Project

Design a Slot - Fed Microstrip Patch Antenna

Operating at 35 GHz

Under Supervision of Prof.: **Islam A. Eshrah**

CU Website: http://scholar.cu.edu.eg/?q=ieshrah/

Dept Website: http://eece.cu.edu.eg/~ieshrah/

TEAM MEMBERS (3rd Year Electronics and Electrical Communication Engineers)	
مجدي أحمد عباس عبد الحميد الابرق	Sec: 3 / I.D: 9210899 / BN: 36
كريم ايمن محمد فخر الدين محمد علي	Sec: 3 / I.D: 9210836 / BN: 26
علي مختار علي الدهشوري	Sec: 3 / I.D: 9210688 / BN: 3
عمر أحمد عبد الكريم عبد الظاهر	Sec: 3 / I.D: 9210705 / BN: 8
مازن وائل ضياء الدين احمد رأفت	Sec: 3 / I.D: 9210892 / BN: 35
علي مصطفي على مصطفي	Sec: 3 / I.D: 9210689 / BN: 4

❖Table of Contents: -

❖ Table of Figures: -

1. Framework

1.1. Abstract:

Microstrip patch antennas are widely utilized in Point-to-Point **(P2P)** communication links, particularly in applications requiring compact design, directional radiation, and flexibility in frequency bands. Their compact size makes them suitable for integration into communication terminals, while their directional radiation patterns enhance the efficiency of P2P links. Additionally, the antennas can be easily customized for various frequency bands, allowing adaptation to the specific requirements of different wireless communication systems. In P2P scenarios, microstrip patch antennas offer advantages such as cost-effectiveness, ease of integration, and reliable performance.

Furthermore, slot-feeding enhances the capabilities of microstrip patch antennas in P2P communication links, especially when targeting the Ka-band frequencies ($\mathbf{26.5 - 40\ GHz}$), such as those used in **5G** applications. Slot-feeding contributes to improved bandwidth, reduced back radiation, enhanced impedance matching, and refined radiation characteristics. This feeding technique is particularly beneficial for achieving better performance metrics, such as a wider bandwidth, lower return loss (S11), and directional beams. As a result, slot-fed microstrip patch antennas prove to be versatile and efficient for applications requiring moderate gains, making them suitable for various P2P communication scenarios, including wireless backhaul, point-to-point links, and millimeter-wave communication.

It's desired to design a **35 GHz** Microstrip patch antenna to serve the **(P2P)** communication links application in the Ka-band.

1.2. Introduction:

Microstrip antennas (MSA) became widely accepted in the 1970's although the first designs and theoretical models appeared in the 1950's. They are suitable for many mobile applications: handheld devices, aircraft, satellite, missile, etc. The MSA are low profile, mechanically robust, inexpensive to manufacture, compatible with MMIC designs and relatively light and compact. They are quite versatile in terms of resonant frequencies, polarization, pattern, and impedance [1].

Some of the limitations and disadvantages of the MSA are:

- Relatively low efficiency (due to dielectric and conductor losses).
- Low power.
- Spurious feed radiation (surface waves, strips, etc.).
- Narrow frequency bandwidth for simple patch geometries (at most a couple of percent).
- Relatively high level of cross polarization radiation.

1.3. Problem Definition:

1.3.1. MSA and their feeding Mechanisms:

The increased interest in the monolithic integration of microstrip antennas with matching networks, amplifiers, phase shifters etc. has led to many new configurations used to feed microstrip antennas. Among them are the four most popular types, namely, the microstrip line, coaxial probe, proximity coupling and aperture coupling. The microstrip line and the coaxial probe feed are classified under the group of direct contact feeding methods while the proximity coupling, and the aperture coupling are grouped under the non-contact feeding method. The non-contact type of feeding method is introduced to counteract some disadvantages, like bandwidth limitation, of the direct contact feeding method.

1.3.2. Aperture Coupled Feed:

The aperture coupled microstrip patch antenna (ACMPA) is of great interest since it allows for the separation of the radiating element (the micro-strip patch) and the feed network ($50\ \Omega$ microstrip transmission line) with a conductive layer (ground) between them.

The micro-strip antenna is formed on a separate dielectric slab above the ground plane and the two structures are electromagnetically coupled through a narrow aperture in the ground plane. The aperture coupled antenna offers many advantages over the conventional direct feed antennas. These include shielding of antenna from spurious feed radiation, use of different substrate for feed structure and antenna if needed, and high bandwidth. It's used in various applications such as satellite and radar communications due to their low cost, thin profile and robustness [2].

In this type of feed technique, the radiating patch and the microstrip feed line are separated by the ground plane as shown in Figure 1. Coupling between the patch and the feed line is made through a slot or an aperture in the ground plane [3].

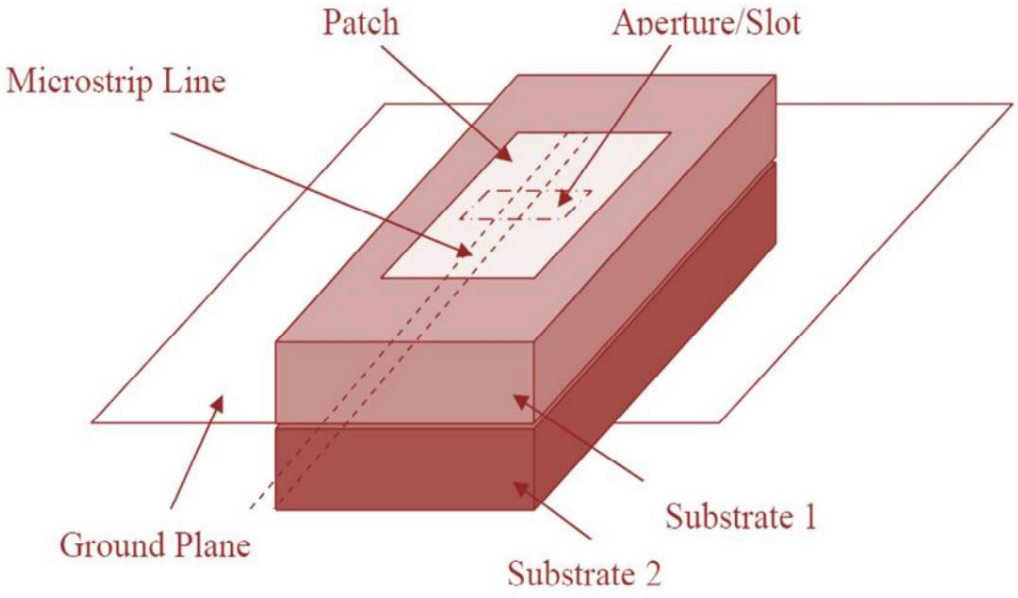

Figure 1: Aperture - Coupled Feed

2. Design Procedure

2.1. Rectangular slot fed microstrip patch antenna - based design:

2.1.1. Concept of patch antenna operation and rectangular geometry:

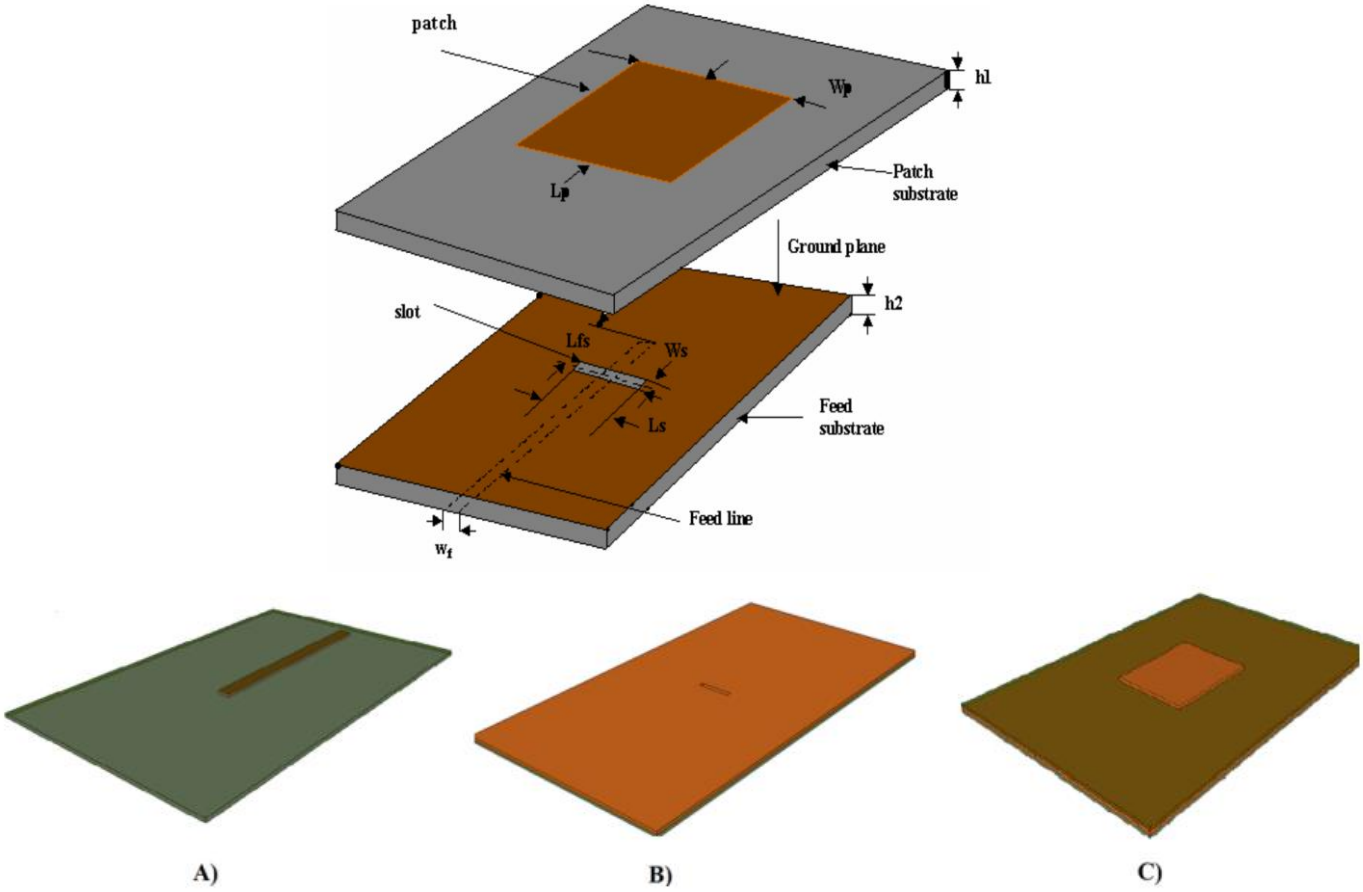

Figure 2: Slot fed microstrip patch antenna layers.

A) Conductive microstrip feed (1st layer) underneath feed substrate (2nd layer).

B) Slotted ground plane (3rd layer). C) Radiating patch (5th layer) on antenna substrate (4th layer).

The rectangular patch geometry as shown in figure 2 is by far the most widely used configuration. It is very easy to analyze using both the transmission-line and cavity models, which are most accurate for thin substrates. We begin with the transmission line model because it is easier to illustrate and also used for its high performance in decreasing the fringing effect as discussed in section 2.1.2. [2]

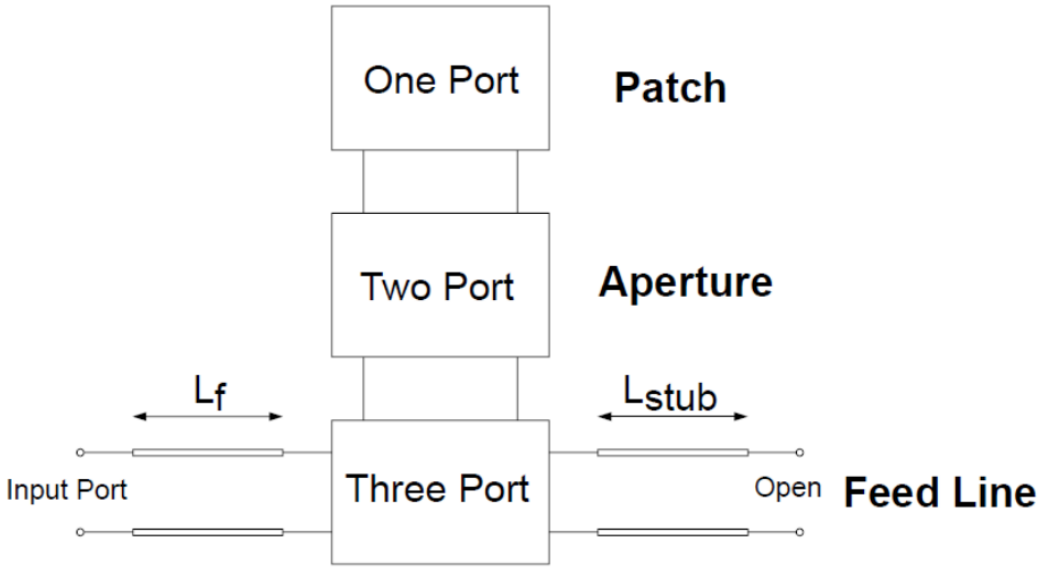

Figure 3: Aperture coupled microstrip antenna block diagram.

The operation of the antenna structure as shown in the block diagram in figure 3 that the feed line creates an electric field in the aperture (ground plane slot), which induces surface currents on the patch effected by the slot which changes in the antenna parameters such as the BW, gain, radiation pattern, etc... Therefore, Changing the slot properties would improve antenna parameters.

The **Feedline Layer** excites power with a 50 Ω transmission line with a nominal value for its Length and width and extended with extra length (L_{stub}) to achieve a certain impedance matching.

The **Aperture Layer** contains the ground layer with a slot fed subtract from it that controls the antenna parameters like gain, BW, radiation pattern, etc. with a nominal dimension for its length and width.

The **Patch Layer** is to direct the power in order to acquire the required antenna parameters.

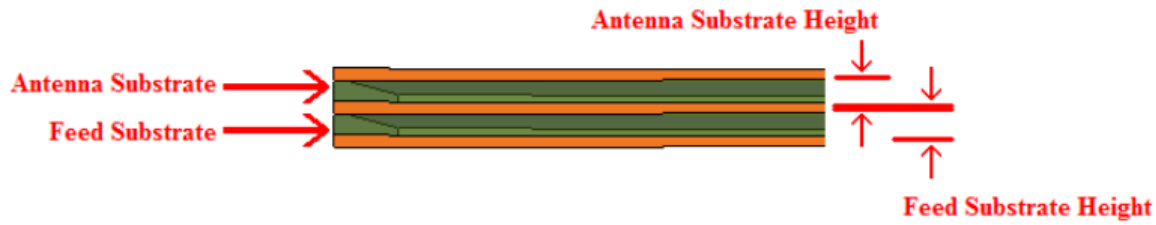

Figure 4: Aperture coupled antenna substrates.

The choice of **Substrate layer** is Rogers RT/Duroid 5880 (tm) substrate, with dielectric loss tangent 0.0009, relative permittivity 2.2 and height 0.25 mm is due to its good performance at high frequency [4].

2.1.2. Design non idealities:

- The initial design assumes certain conditions as perfect electric conditions that eliminates the electrical extensions.

- Edging contact and fringing effects:

  The advantage of this design is the use of coupling mechanism (non-contact feeding) which suppresses any potential losses due to the edge contact.

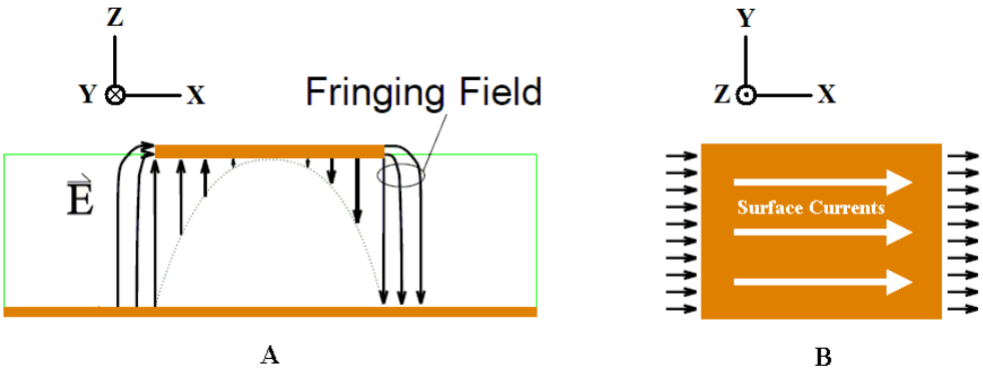

Figure 5: Patch electric fringing fields A) Side view (at y=0) B) Top view.

- The patch edges perpendicular to the feed line create fringing fields that radiate into free space. A microstrip patch antenna would look electrically wider compared to its physical dimensions. As shown in figure 5, waves travel both in substrate and in the air. Thus, an effective dielectric constant $\epsilon_{r_{eff}}$ is to be introduced. The effective dielectric constant $\epsilon_{r_{eff}}$ takes in account the fringing and the wave propagation in the line [5].

❖ The initial design has been proceeded with the nominal values considering the ideal conditions then we tuned the parameters to counter act the latter non-idealities for copper conductors with minimal thickness as will be shown in the table in the next section [6].

- All metals including patch, ground and feed line was chosen to be in copper with thickness equals 35 microns.

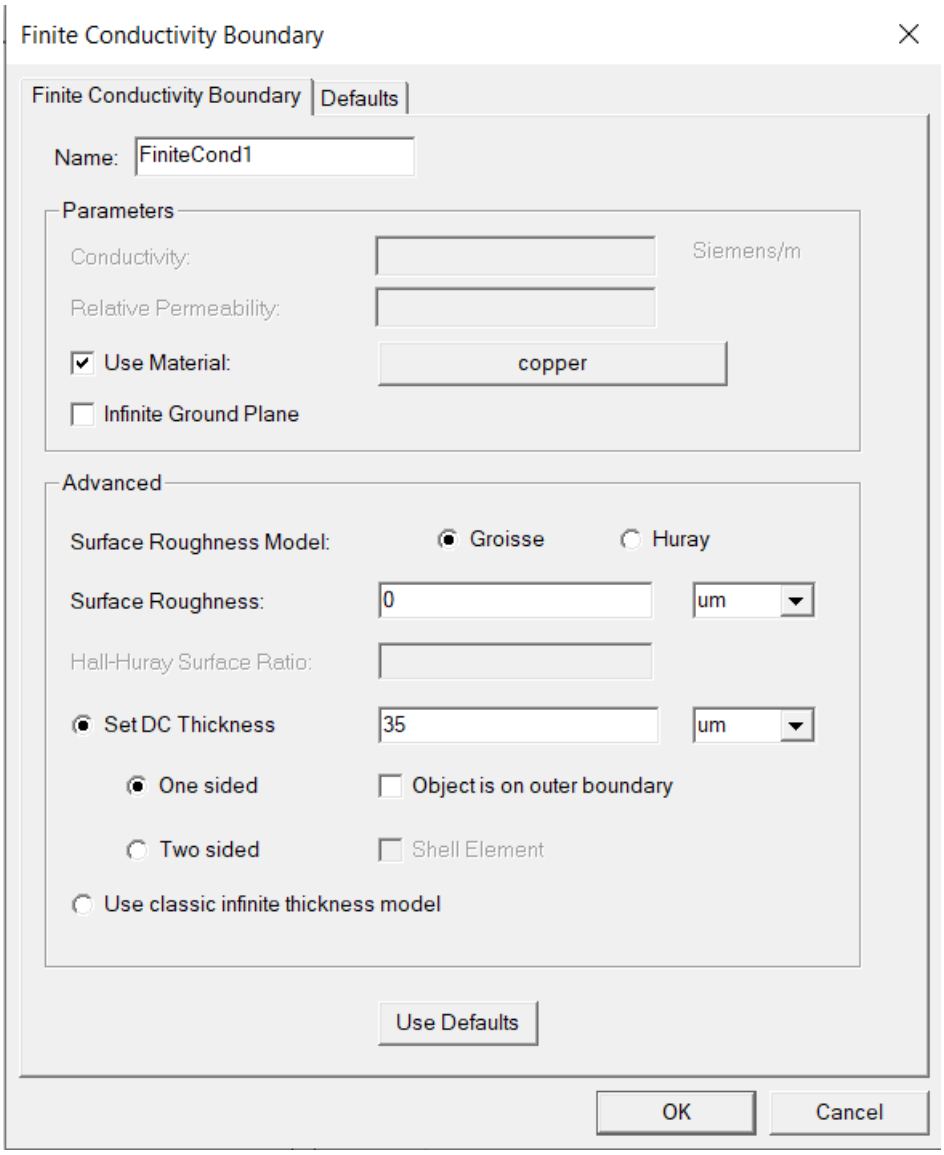

Figure 6*: Copper conductors*

2.1.3. Design Scheme:

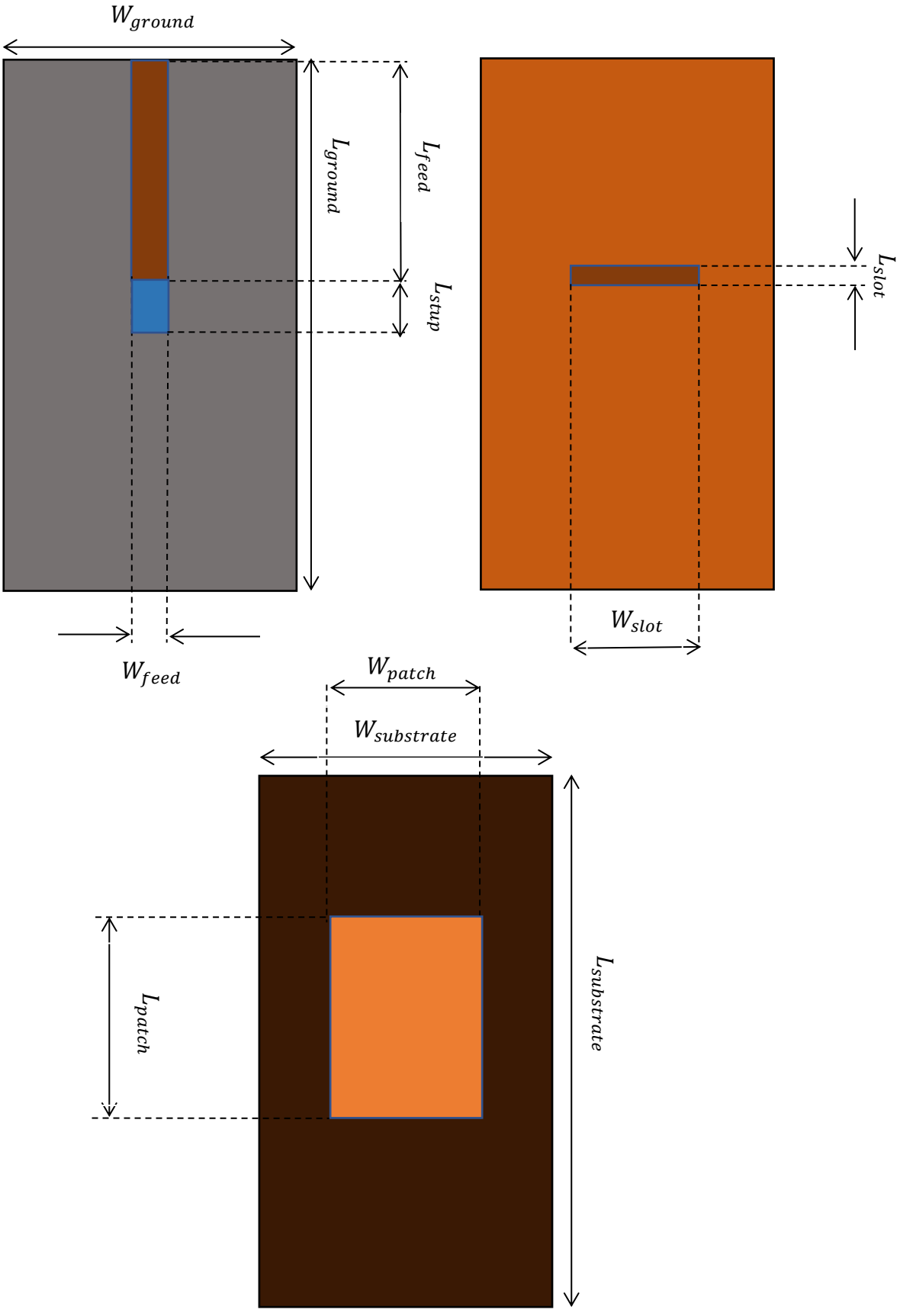

Table 1: Antenna Dimensions

Dimensions and Equations for Antenna Knobs		
Dimensions	**Nominal values (mm)**	**Tuned values (mm)**
$\mathbf{L_{substrate} = L_{ground}}$	$L_{patch} + 6H_{sub} = 4.2425$	4.2425
$\mathbf{W_{substrate} = W_{ground}}$	$W_{patch} + 6H_{sub} = 4.882$	4.882
$\mathbf{H_{substrate}}$	$\left(H_{sub} \leq \frac{0.3c}{2\pi f_{res}\sqrt{\epsilon_r}}\right) \rightarrow 0.25$	0.2815
$\mathbf{L_{feed}}$	$\frac{L_{sub}}{2} + L_{stub} = 3.566$	3.9225
$\mathbf{W_{feed} = W_{source}}$	line Calculator $(50\ \Omega) \rightarrow 0.385$	0.385
$\mathbf{H_{source}}$	$\frac{H_{sub}}{2} = 0.125$	0.14075
$\mathbf{H_{ground}}$	$H_{sub} = 0.25$	0.2815
$\mathbf{L_{patch}}$	$L_{eff} - 2\Delta L = 2.7425$	2.5535
$\mathbf{W_{patch}}$	$\frac{c}{2f}\sqrt{\frac{2}{\epsilon_r + 1}} = 3.3882$	3.193
$\mathbf{L_{slot}}$	$0.13\lambda_o = 1.142$	1.02098
$\mathbf{W_{slot}}$	$0.1\lambda_o = 0.85714$	0.85714
$\mathbf{L_{stub}}$	$\frac{\lambda_r}{4} = \frac{\lambda_0}{4\sqrt{\epsilon_r}} = 1.447$	1.801
Thickness For Feedline, Patch & ground	0.035	0.035
Electrical Extension	$\Delta L = 0.412\ H_{sub} \frac{\left(\epsilon_{r_{eff}}+0.3\right)\left(\frac{W_{sub}}{H_{sub}}+0.264\right)}{\left(\epsilon_{r_{eff}}-0.258\right)\left(\frac{W_{sub}}{H_{sub}}+0.8\right)} = 0.13025, \frac{W_{sub}}{H_{sub}} > 1$	
Effective Length & Effective Permittivity	$L_{eff} = \frac{c}{2f\sqrt{\epsilon_{eff}}} = 3\ , \epsilon_{r_{eff}} = \frac{\epsilon_r+1}{2} + \frac{\epsilon_r-1}{2}\left[1 + 12\frac{H_{sub}}{W_{sub}}\right]^{-\frac{1}{2}} = 2.037$	

3. Results and Discussion

3.1. Verification of EM tool:

To validate the functionality of the HFSS electromagnetic tool, we aim to construct a lambda over two dipole. This involves computing the radiation impedance and analyzing the radiation pattern, anticipating that it aligns closely with the theoretical predictions.

3.1.1. Design:

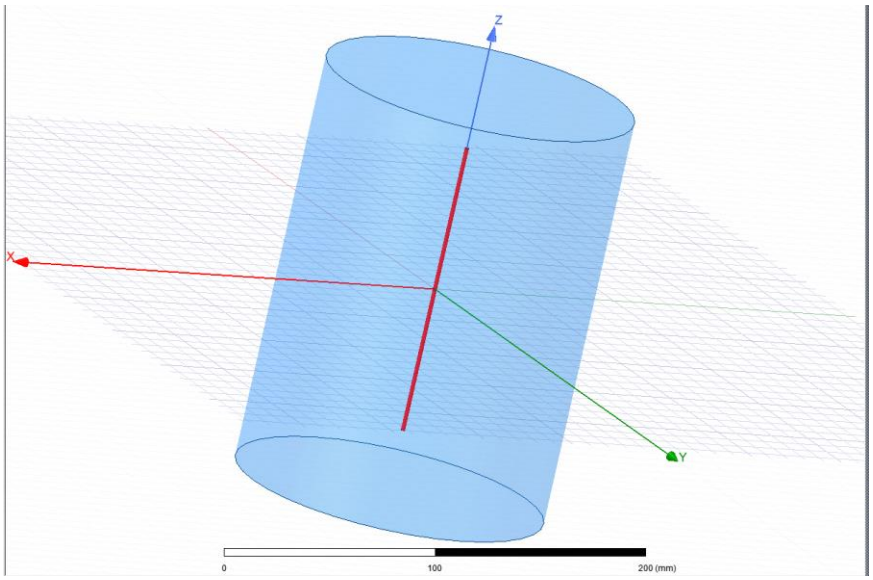

Figure 7: Lamda over two dipole.

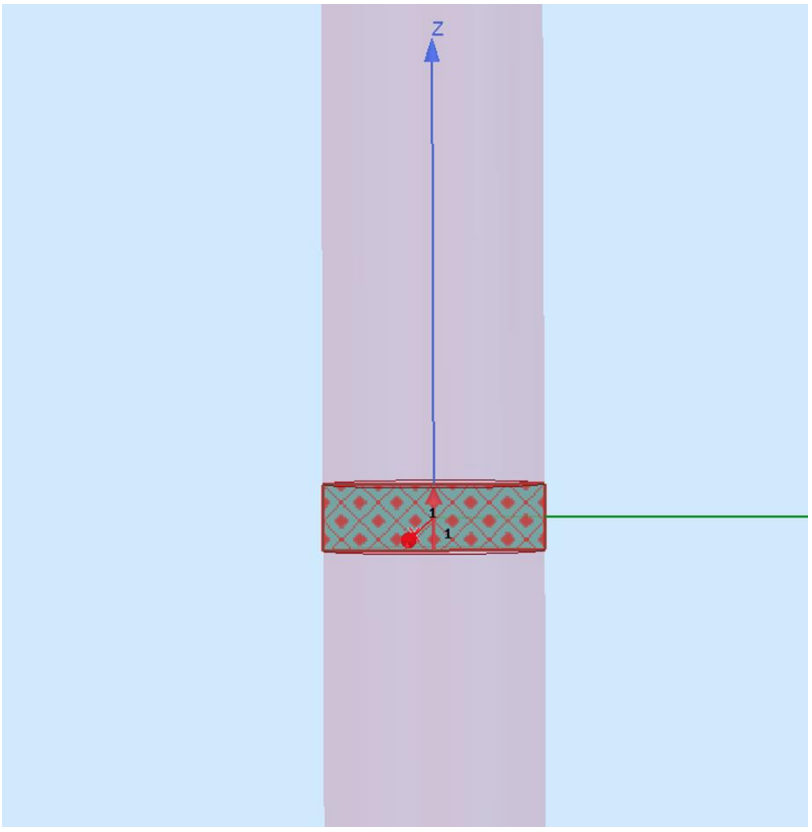

Figure 8: Port Excitation

The intention was for the dipole to function at $1\ GHz$, correlating to a wavelength of $300\ mm$. Therefore, the total length of the dipole was selected to be roughly 0.48 times the wavelength.

- $R_{radiation} = 60\ R(x)$

Using the provided equation, the actual radiation resistance, calculated at $x = (\pi L)\ as\ L = \frac{\lambda}{2}$, stands at $60\ \Omega$ times $R(x)$. Substituting the value into the equation yields $R(x) = 1.21883$. Consequently, the anticipated radiation resistance, denoted as $R_{radiation}$, at the resonance frequency, is expected to be around $73.1298\ \Omega$.

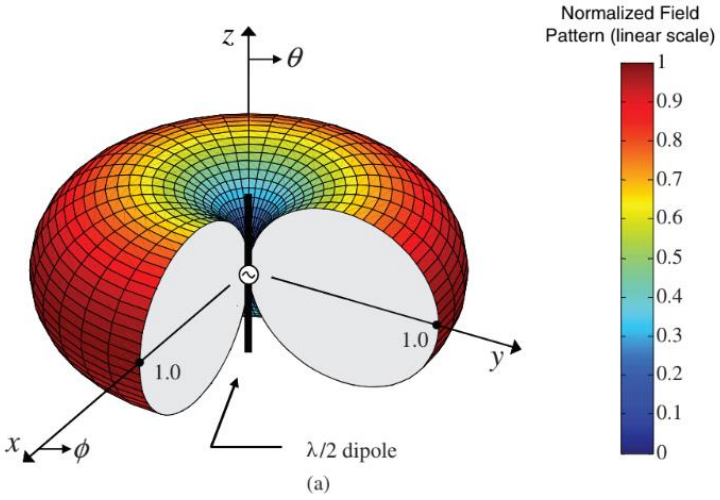

Figure 9: Expected Radiation Patten

3.1.2. Results:

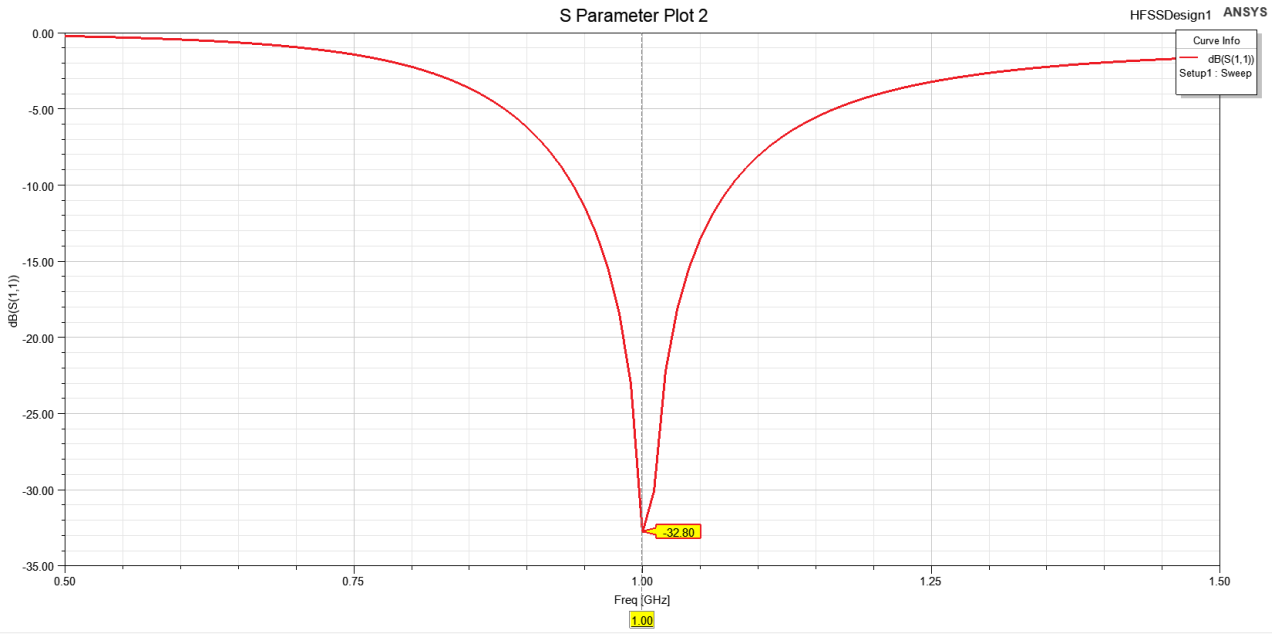

Figure 10: Return Loss S11

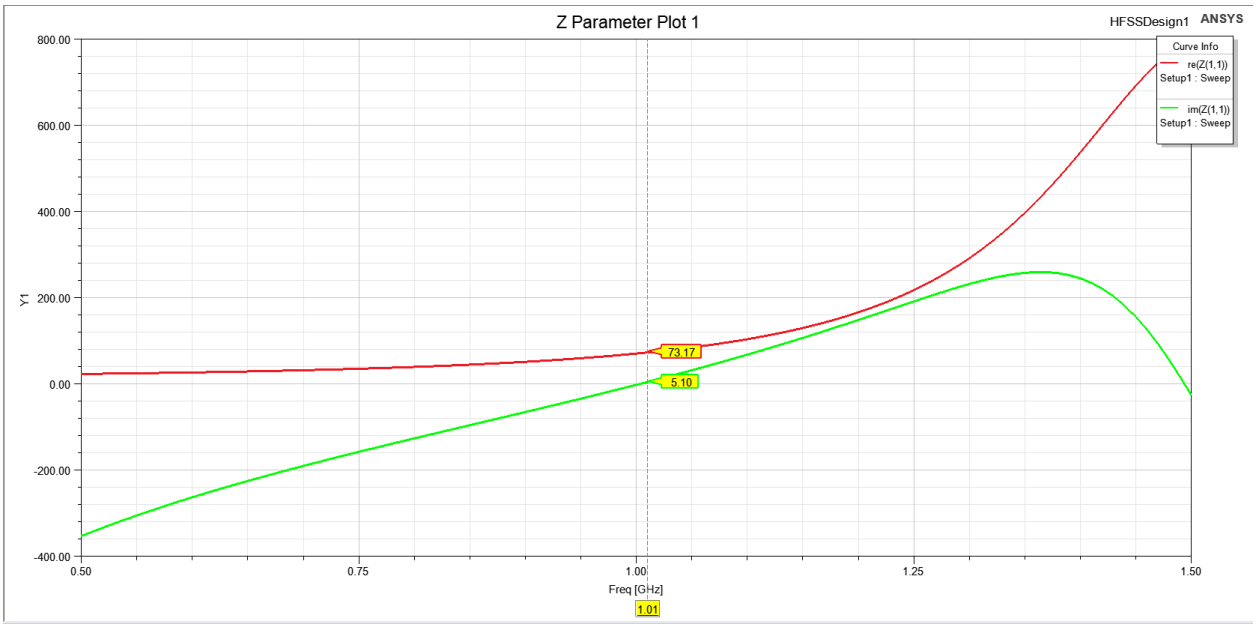

Figure 11: $R_{radiation}$

The dipole antenna has attained a return loss of -32 dB at 1 GHz, indicating effective impedance matching, as depicted in figure 6. Additionally, at 1.01 GHz, the real part of the radiation resistance stands at 73.17 ohms, aligning closely with the theoretical value, illustrated in figure 10 and 11.

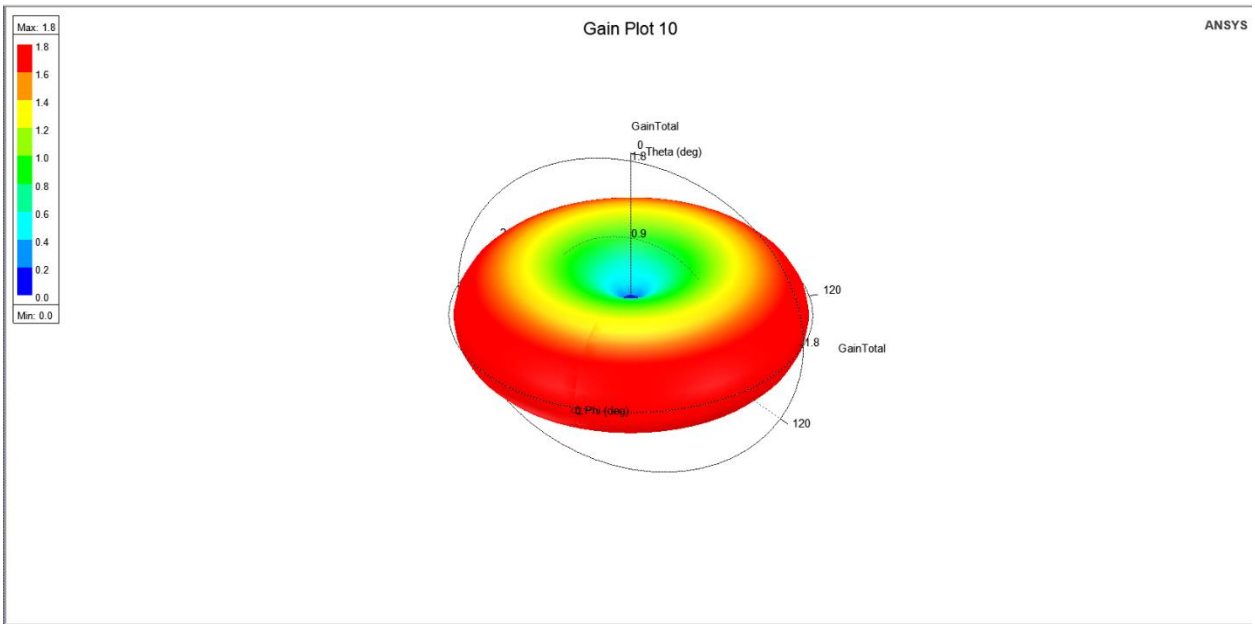

Figure 12: 3D Radiation Pattern

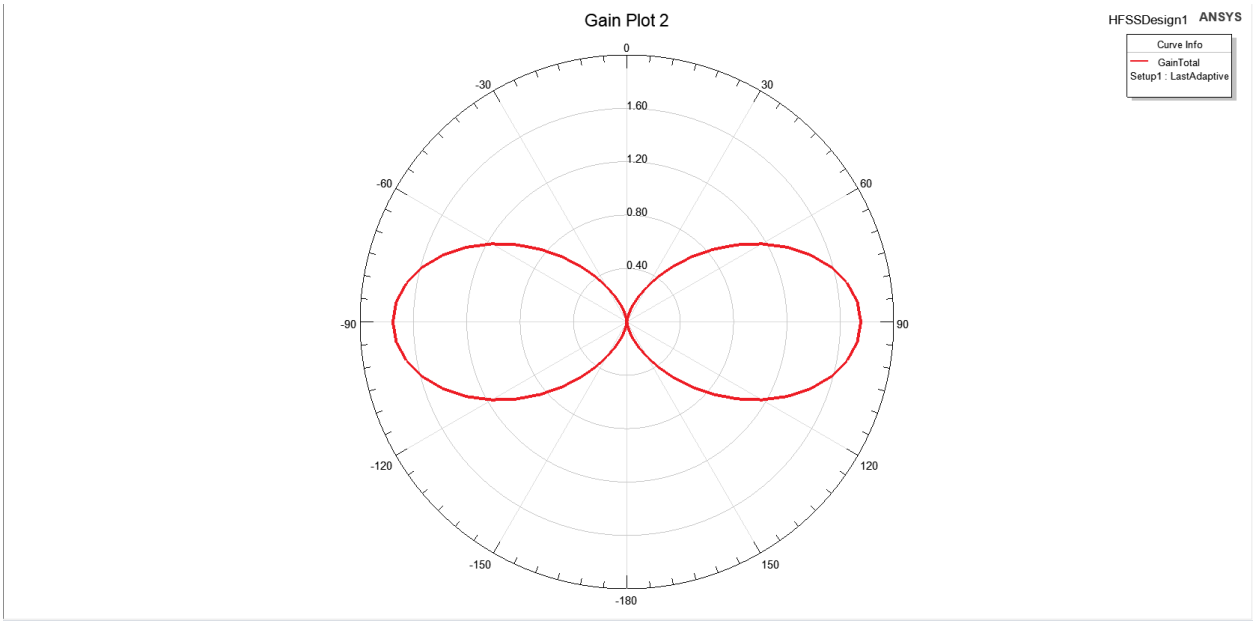

Figure 13: E - Plane

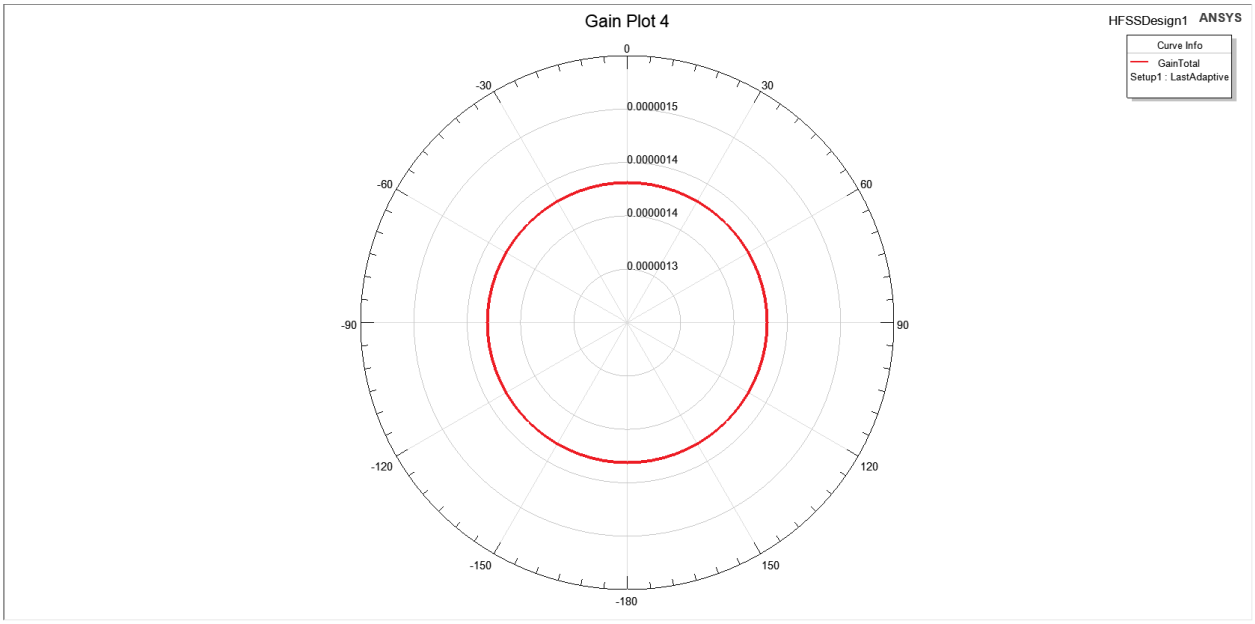

Figure 14: H – Plane

The dipole antenna exhibited the anticipated radiation pattern, aligning with the teachings of the course. This pattern includes maximum gain occurring at theta = 90 degrees in the E-plane and a consistent circular shape in the H-plane, showing no variation with phi.

3.1.3. Conclusion:

The successful alignment of the designed dipole antenna with the theoretical values indicates the completion of the verification phase. This achievement demonstrates the accurate functionality and proper execution of HFSS, affirming its reliability in accurately modeling and predicting antenna performance.

3.2. Simulations and Analysis:

This section consolidates design, simulation, and fabrication efforts for the slot-fed antenna, emphasizing its 35 GHz performance. The analysis evaluates real results against expectations to gauge high-frequency suitability. Detailed scrutiny includes radiation patterns and impedance matching, studying their impact on the antenna at 35 GHz.
The antenna is being analyzed with respect to:
1 - System-level considerations e.g.: Matching
2 - Antenna & Radiation Characteristics e.g.: polarization
3 - practical use-case e.g.: Radiation Efficiency

3.2.1. Return Loss:

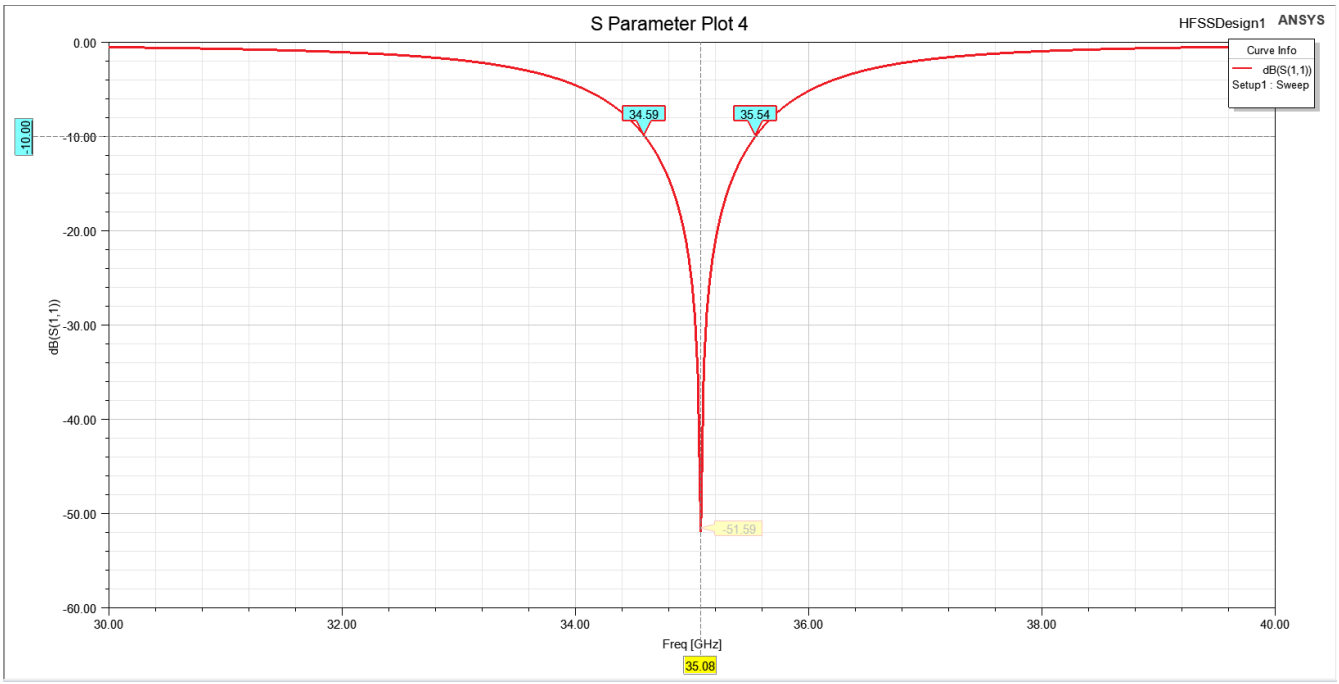

Figure 15: Return Loss S11

Achieving a return loss of -52 dB at 35.08 GHz, accompanied by a bandwidth of 0.95 GHz, signifies robust impedance matching and operational versatility, ensuring minimal signal reflections and a wide operational frequency range for diverse communication applications, shown in figure 15.

3.2.2. Input Impedance:

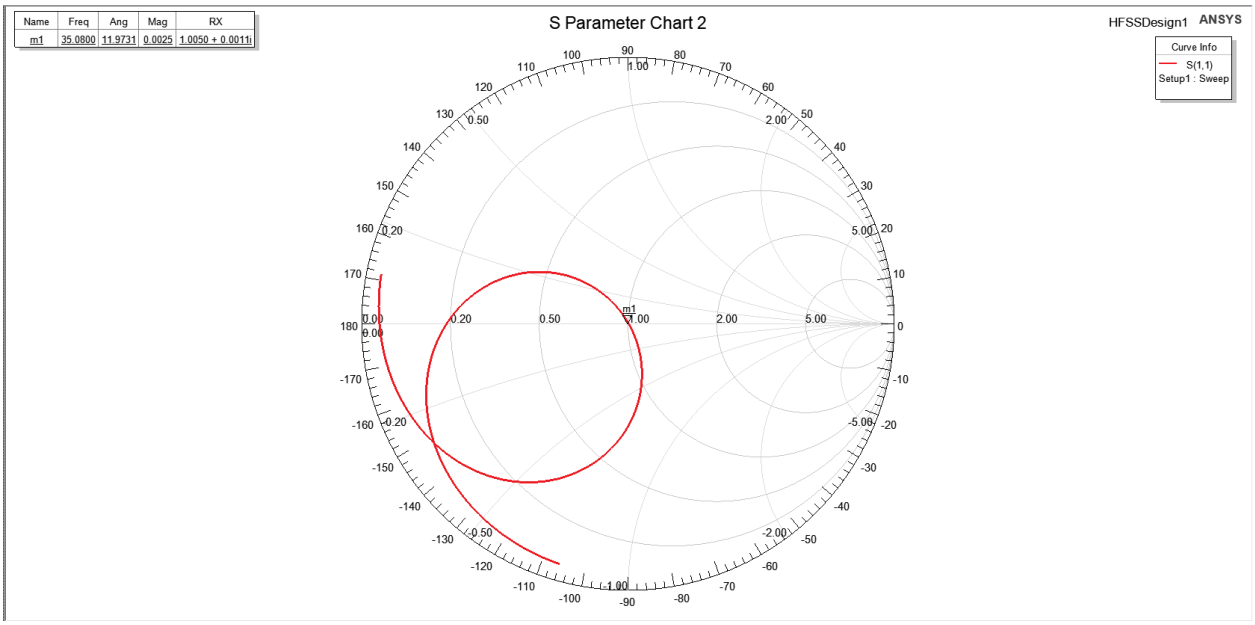

Figure 16: Input Impedance

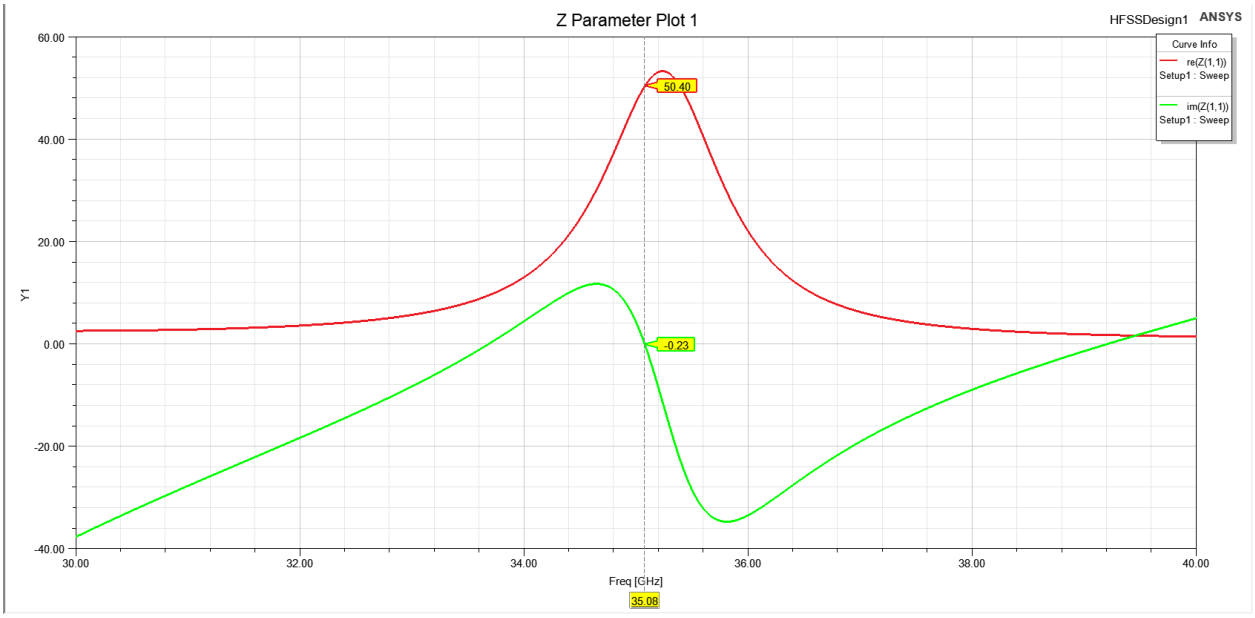

Figure 17: Real and imaginary part of input impedance

Attaining an input impedance of 50.8 ohms at 35.08 GHz signifies excellent matching, aligning seamlessly with standard requirements for optimal power transfer and signal integrity within the specified frequency range, shown in figure 16 and 17.

3.2.3. The Radiation Pattern in E and H Planes:

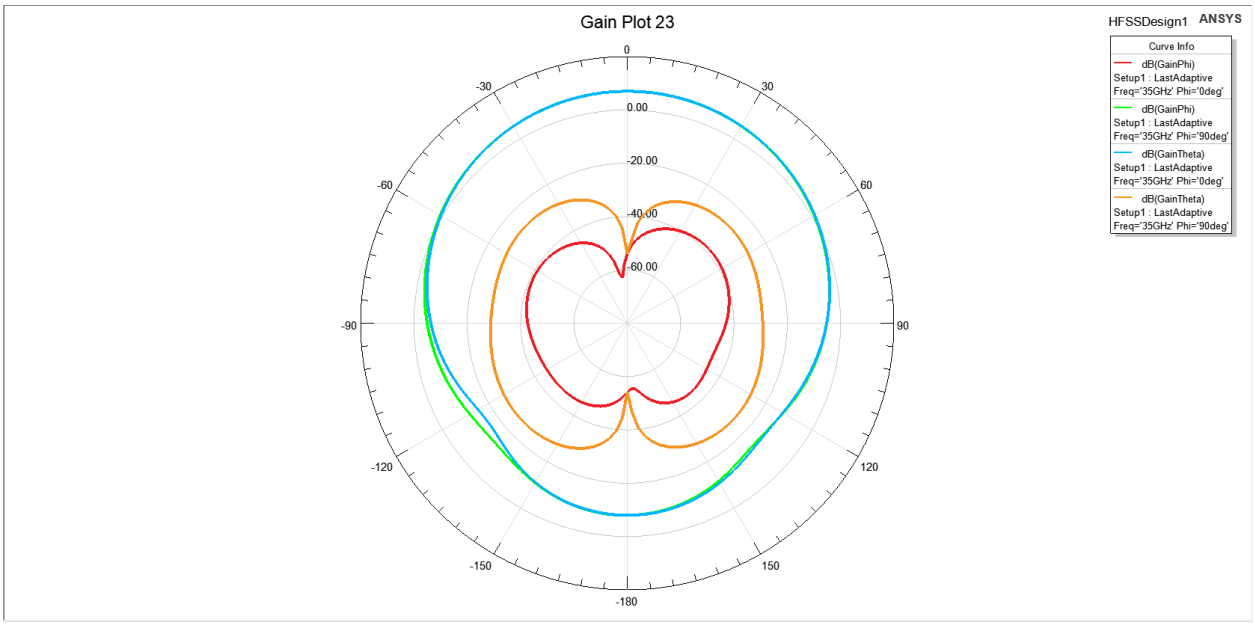

Figure 18: E and H planes

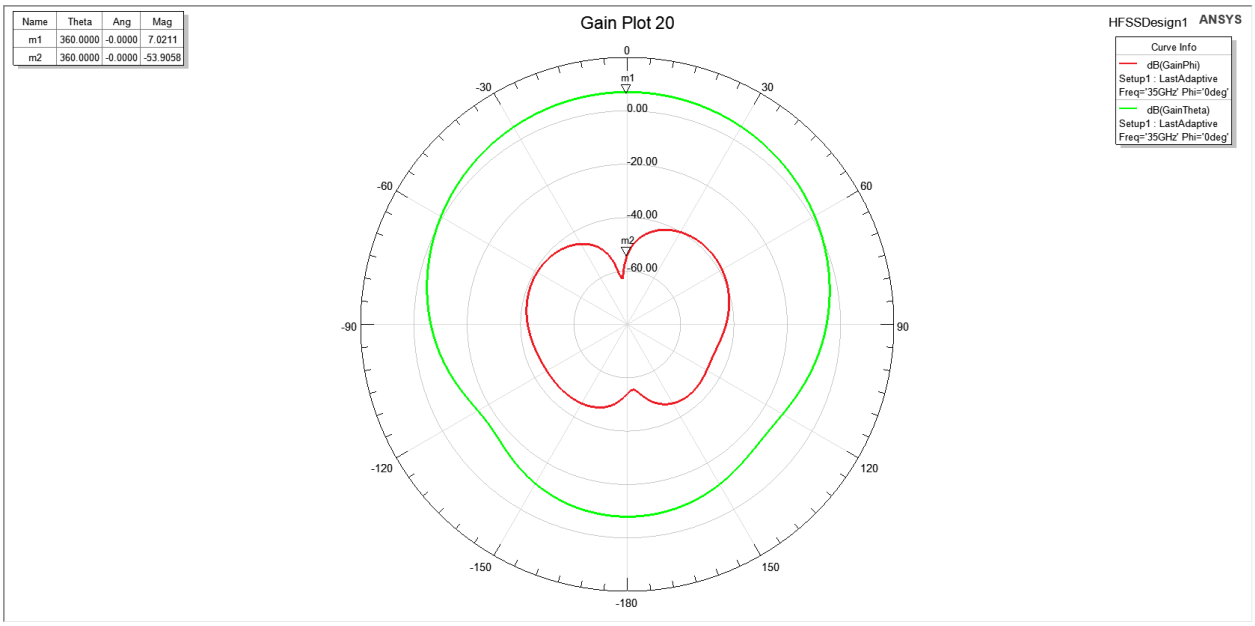

Figure 19: E Plane

The alignment of the feed line parallel to the x-axis resulted in current flow along the x-direction, positioning the E-plane within the XZ plane at a phi of zero degrees.
The antenna achieved a peak co-polarization of 0 dB and a cross-polarization of -53.9 dB in E-plane at a maximum of theta 360 degrees, showcasing a favorable outcome in radiation pattern characteristics, shown in figure 18 & 19.

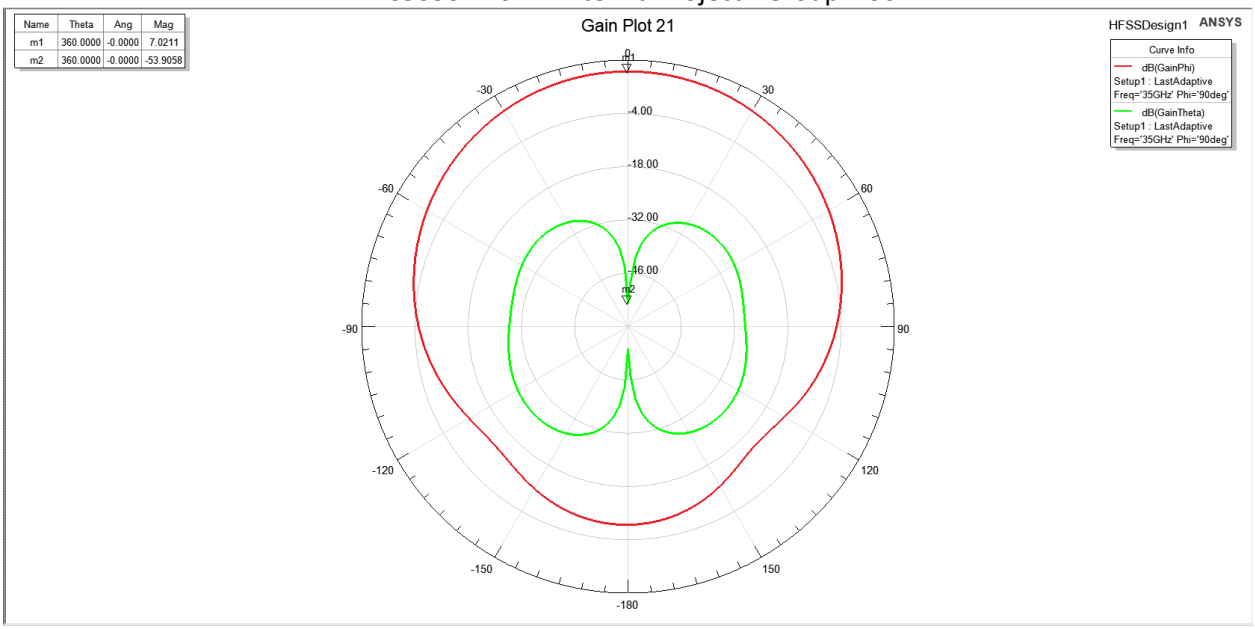

Figure 20: H Plane

The alignment of the feed line parallel to the x-axis resulted in current flow along the x-direction, positioning the H-plane within the YZ plane at a phi of 90 degrees. The antenna achieved a peak cross -polarization of 0 dB and a co-polarization of -53.9 dB in H-plane at a maximum of theta 360 degrees, showcasing a favorable outcome in radiation pattern characteristics, shown in figure 20.

3.2.4. The Gain and Radiation Efficiency:

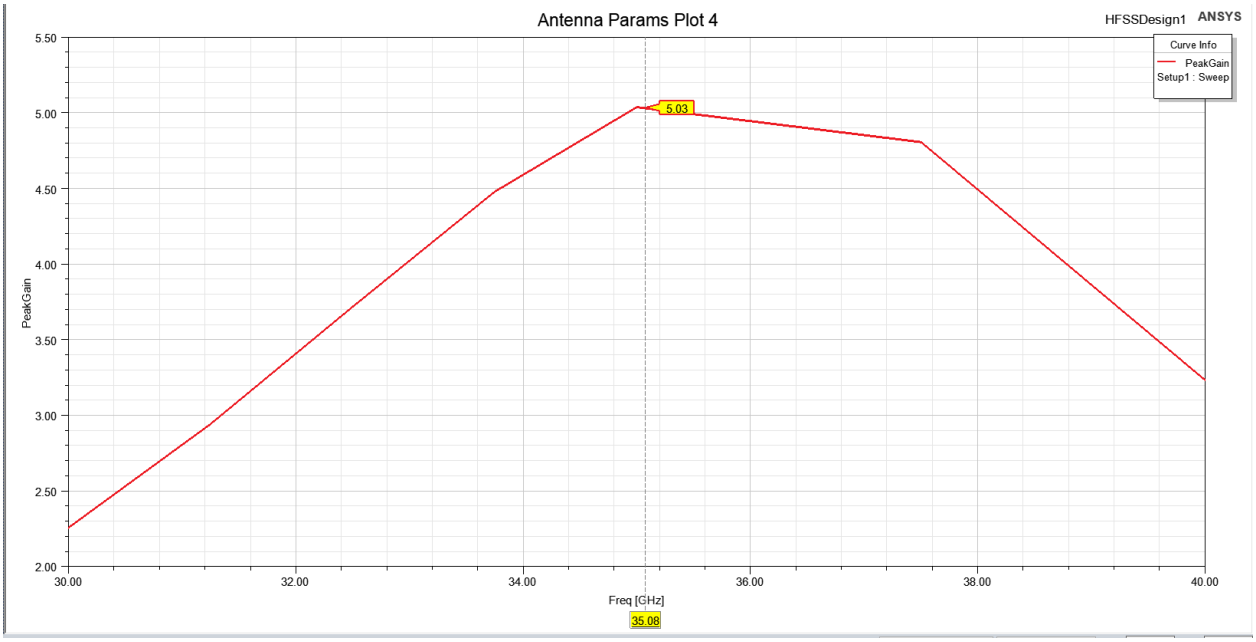

Figure 21: Gain vs Frequency

Securing a gain of 5.3 at 35.08 GHz signifies a commendable directional efficiency, demonstrating the antenna's ability to focus and amplify signals in the desired direction, essential for targeted and robust signal transmission within the specified frequency range, shown in figure 21.

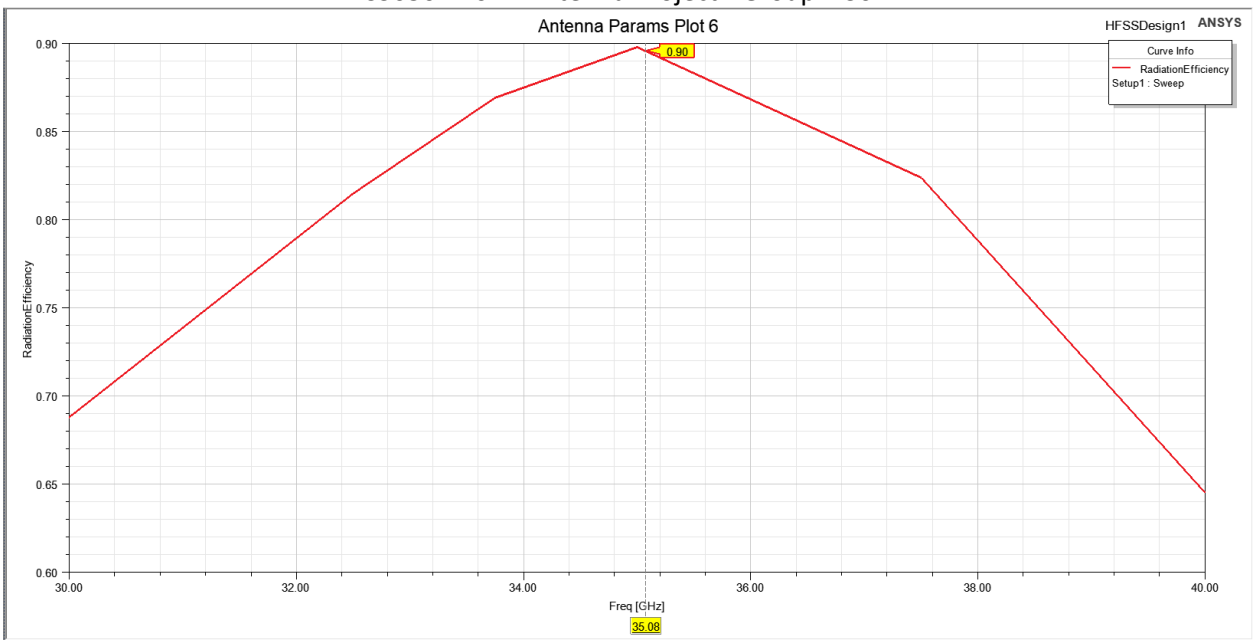

Figure 22: Radiation Efficiency vs Frequency

Obtaining a radiation efficiency of 0.9 at 35.08 GHz showcases an impressive utilization of input power for radiation, indicating minimal losses and maximizing the antenna's effectiveness in converting input power into useful radiated energy within the specified frequency band, shown in figure 22.

3.2.5. More Characteristics:

3.2.5.1. VSWR:

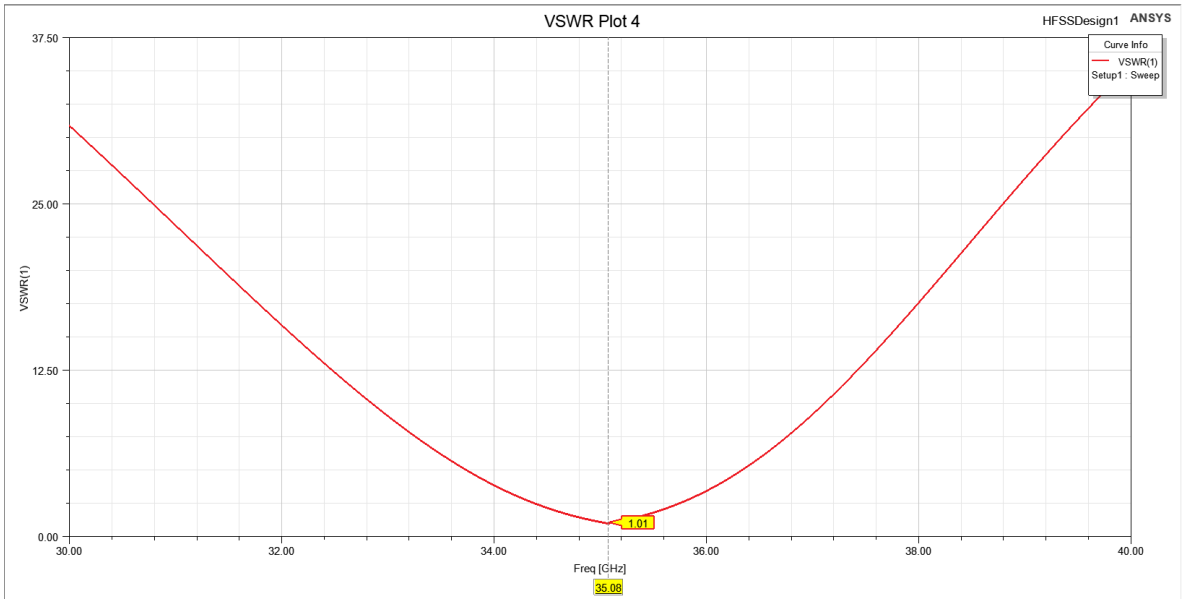

Figure 23: VSWR

Attaining a VSWR of 1.01 at 35.08 GHz signifies exceptional impedance matching and minimal signal loss, reflecting the antenna's remarkable efficiency and suitability for high-frequency applications, ensuring robust signal transmission within the specified frequency range, shown in figure 23.

3.2.5.2. Front to back Ratio:

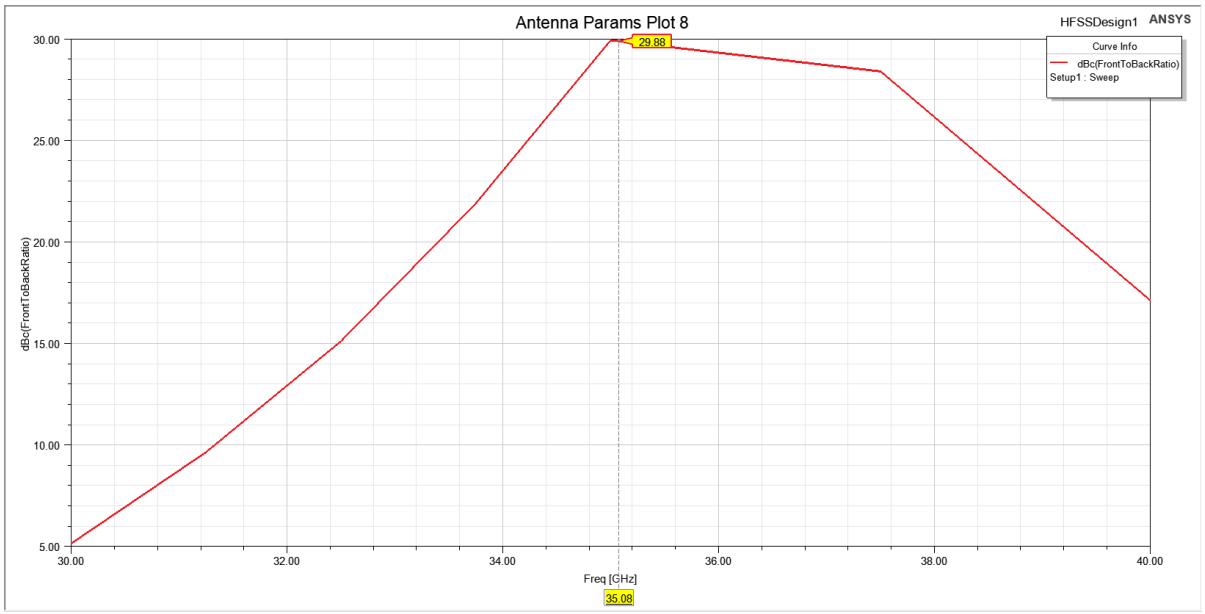

Figure 24: Front to back Ratio

Obtaining a front-to-back ratio of 29.88 dB at 35.08 GHz underscores the antenna's exceptional directional selectivity, highlighting its proficiency in distinguishing and favoring signals from desired directions over undesired ones, critical for signal clarity and interference reduction within the designated frequency range, shown on figure 24.

3.2.5.3. XPD:

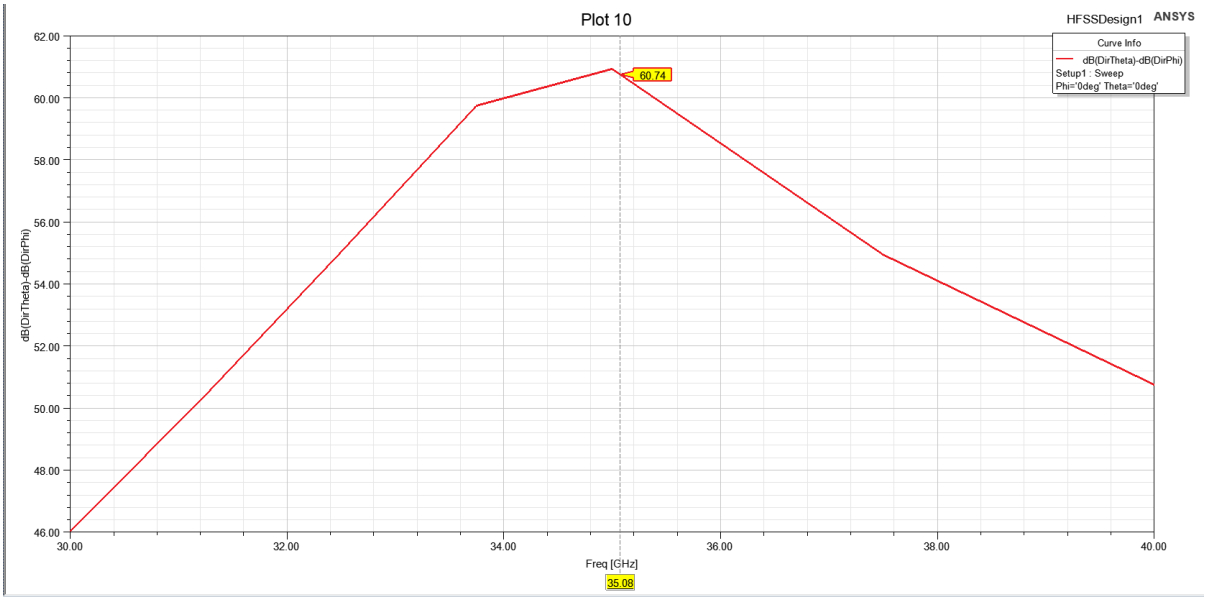

Figure 25: XPD

An XPD of 60.74 dB at 35.08 GHz showcases excellent antenna performance, minimizing signal interference and maximizing clarity in high-frequency communication, shown on figure 25.

3.2.5.4. 3D Gain:

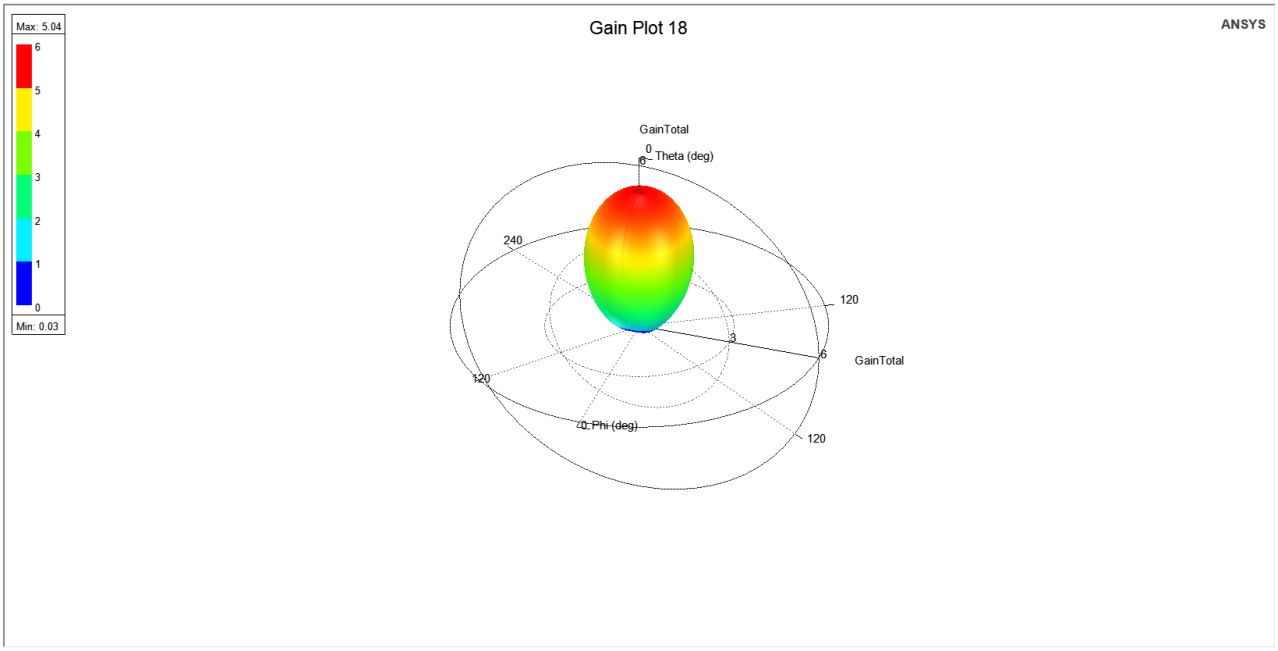

Figure 26: 3D – Gain

3.2.6. Equivalent circuit model - based design:

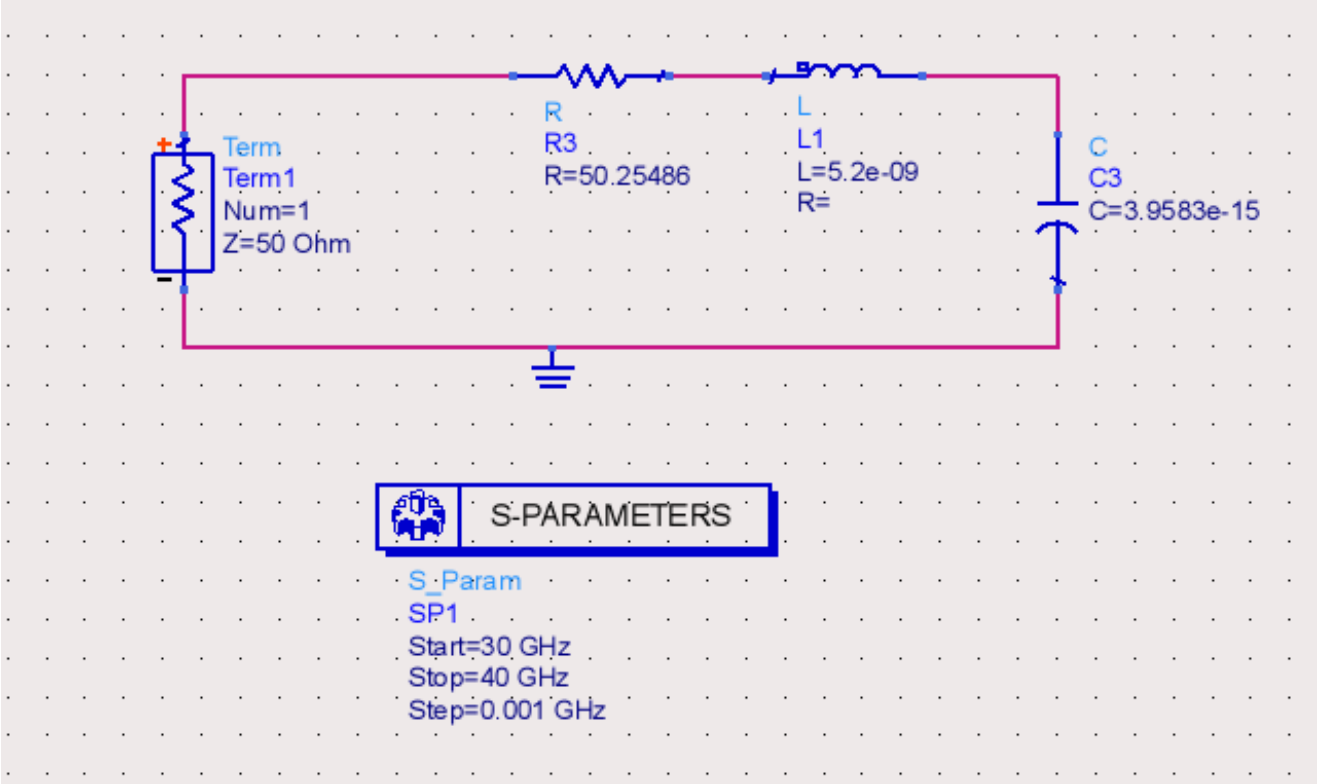

Figure 27: Equivalent Circuit Model

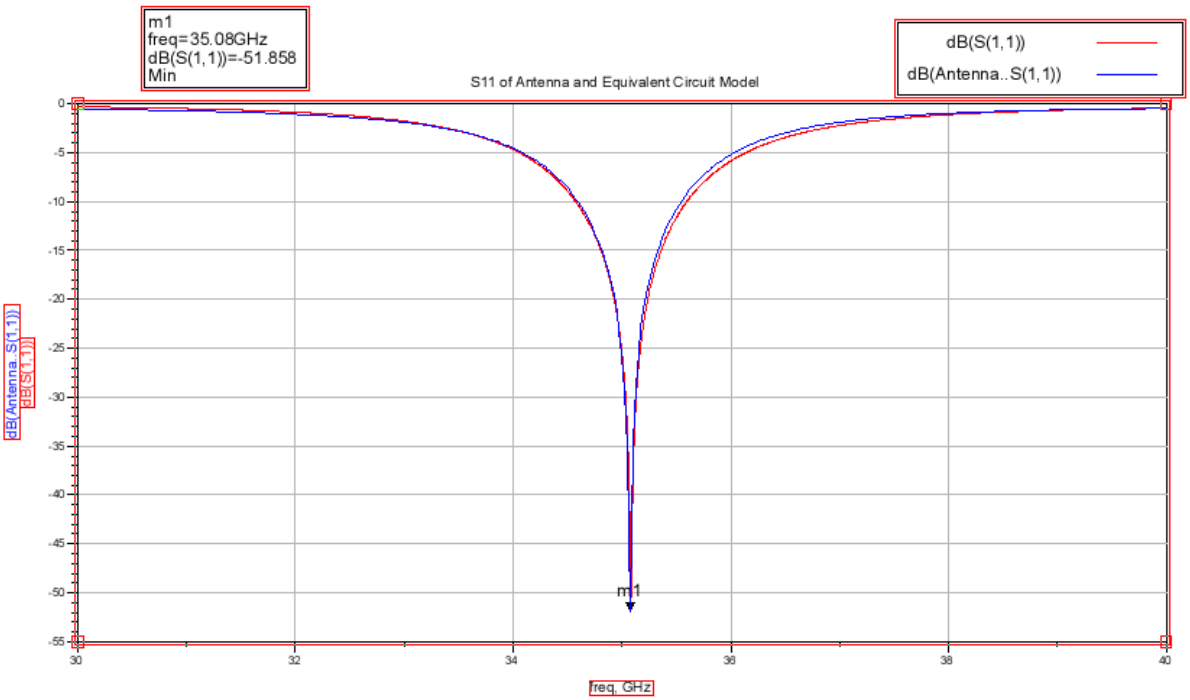

Figure 28: Equivalent S11 (Return Loss)

To replicate the S11 performance at 35 GHz and maintain the identical bandwidth, the initial step involved creating an equivalent circuit model mirroring the slot-fed antenna. This commenced with the formulation of a series RLC circuit, depicted in figure 28.

- $F_s = \frac{1}{2\pi\sqrt{LC}}$
- $S11 = \frac{R-Z_0}{R+Z_0}$
- $BW = \frac{R}{L}$

Based on the equations mentioned earlier, an inductance (L) of 5.2e-9 H and a capacitance (C) of 3.9583e-15 F were selected to center the frequency near 35.08 GHz, aligning with the antenna design. Additionally, the resistance (R) was adjusted to 50.25486 ohms to achieve an S11 of approximately -51.59 dB, consistent with the antenna's performance. The specific values of R and C were determined in consideration of matching the antenna's bandwidth, illustrated in figure 26.

4. Final Design Layout

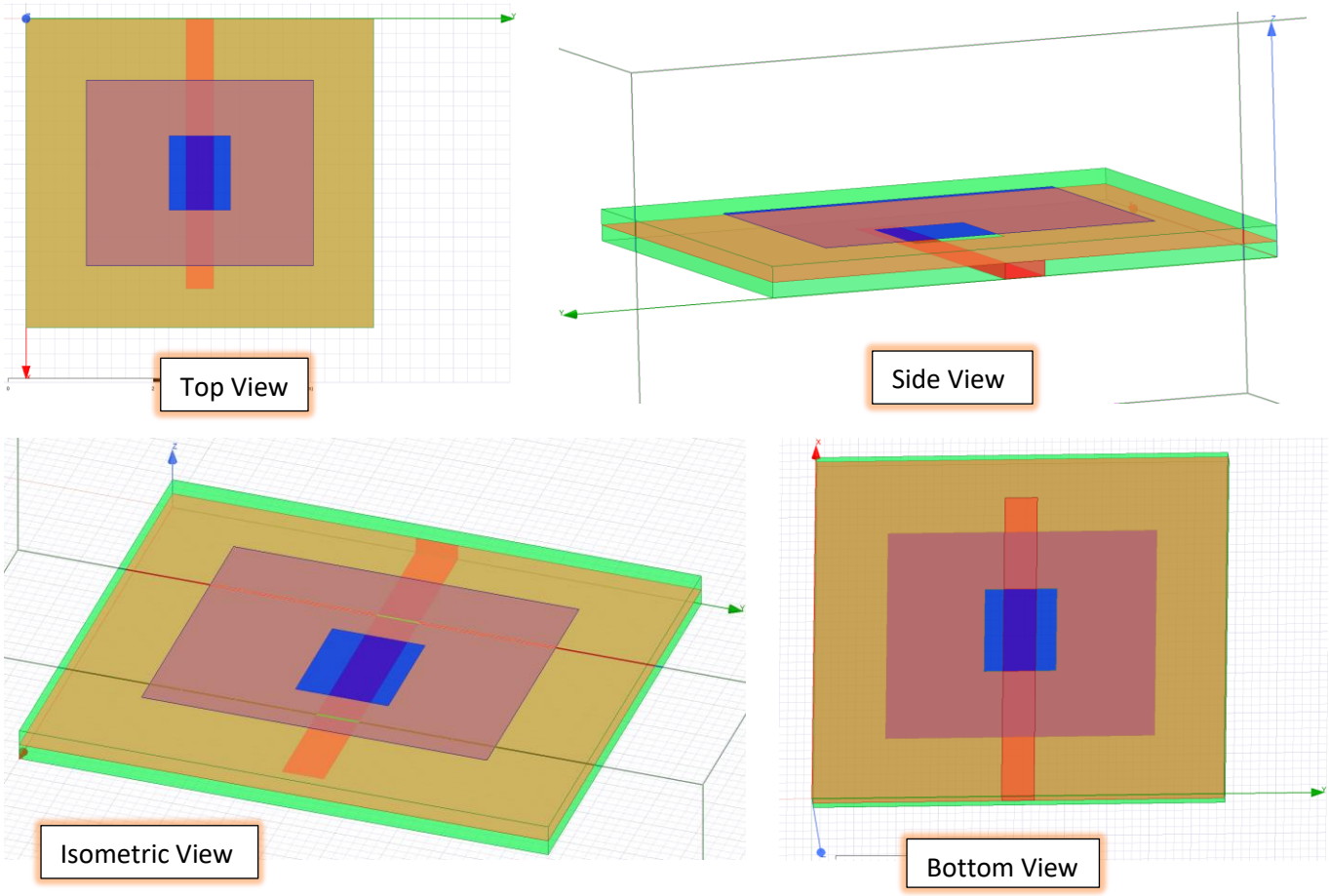

Figure 29: Final Design Layout

The final design layout represents the culmination of meticulous engineering, leveraging precise component values and strategic configurations to mirror the antenna's performance characteristics. Its intricate arrangement embodies a harmonious balance between theoretical precision and practical implementation, ensuring optimal resonance, bandwidth, and impedance matching at the target frequency of 35.08 GHz. This layout stands as a testament to the meticulous attention to detail and iterative refinement in achieving a design that echoes the antenna's superior functionality and performance, illustrated in figure 29.

5. Conclusion

In conclusion, this exhaustive exploration and meticulous design journey have yielded an exemplary slot-fed antenna system, resonating at 35.08 GHz with impeccable precision. Through an intricate balance of theory and practical implementation, we've achieved not just a design, but an embodiment of engineering excellence. This antenna showcases not only superior performance in terms of return loss, bandwidth, and radiation characteristics but also embodies the culmination of relentless refinement and innovation. Its success underscores not just a technical feat, but a testament to the pursuit of pushing boundaries, setting a benchmark for future advancements in high-frequency antenna engineering.

6. References

[1] Lecture 20: Microstrip Antennas - McMaster University.
Available at: (Accessed: 29 December 2023).
https://www.ece.mcmaster.ca/faculty/nikolova/antenna_dload/current_lectures/L20_Mstrip1.pdf

[2] Manoj Singh, Ananjan Basu, and S.K. Koul, "Design of Aperture Coupled Fed Micro-Strip Patch Antenna for Wireless Communication."
Available: https://sci.bban.top/pdf/10.1109/INDCON.2006.302848.pdf

[3] N. Kaur, M. Tech Scholar, N. Sharma, and N. Singh, "A Study of Different Feeding Mechanisms in Microstrip Patch Antenna," International Journal of Microwaves Applications, vol. 6, no. 1, pp. 5–9, 2017, Accessed: Dec. 25, 2023. [Online].
Available: http://www.warse.org/IJMA/static/pdf/file/ijma02612017.pdf

[4] M. P. Civerolo, "Aperture Coupled Microstrip Antenna Design and Analysis," Semantic Scholar, 2010. https://www.semanticscholar.org/paper/Aperture-Coupled-Microstrip-Antenna-Design-and-Civerolo/f36e6547818f642c26c92b9c9a1507b1ad3e3624
(accessed Sep. 25, 2022).

[5] C. A. Balanis, *Antenna Theory*. John Wiley & Sons, 2012.

[6] S.-E. Didi, I. Halkhams, M. Fattah, Y. Balboul, S. Mazer, and M. E. Bekkali, "Design of a microstrip antenna patch with a rectangular slot for 5G applications operating at 28 GHz," *TELKOMNIKA (Telecommunication Computing Electronics and Control)*, vol. 20, no. 3, p. 527, Jun. 2022, doi: https://doi.org/10.12928/telkomnika.v20i3.23159 .